Multidimensional femtosecond spectroscopies of vibrational motions in liquids: Semiclassical expansion

V. Chernyak and S. Mukamel
Department of Chemistry, University of Rochester, P.O. RC Box 270216, Rochester, New York 14627-0216

(Received 2 October 1997; accepted 8 January 1998)

Fifth- ($\chi^{(5)}$) and seventh- ($\chi^{(7)}$) order electronically off-resonant Raman spectroscopies in molecular liquids are investigated using a new semiclassical expansion of the optical response which applies for weak anharmonicities and low temperatures. The leading contribution can be calculated using classical equations of motion for nuclear wave packets, even when the system itself may be highly nonclassical. Two sources of nonlinearities which generate the signals—the nonlinear dependence of the polarizability on nuclear coordinates and vibrational anharmonicities—are identified. Formal analogy between the present equations and the time-dependent Hartree–Fock equations used in electronic nonlinear spectroscopy suggests specific experimental signatures of the various nonlinearities. © *1998 American Institute of Physics.* [S0021-9606(98)50814-8]

I. INTRODUCTION

Time-resolved vibrational spectroscopy is a powerful tool in the studies of intramolecular and intermolecular dynamics of liquids and other condensed phase systems with complex nuclear motions such as proteins, polymers, and glasses.[1] The electronically off resonant coherent anti-Stokes Raman (CARS) technique has long been used for probing vibrational frequencies, relaxation and dephasing rates.[2] Loring and Mukamel have shown that, despite initial claims to the contrary, the technique carries precisely the same information as ordinary spontaneous Raman spectroscopy. (In fact, the two signals are related by a simple Fourier transform.[3]) The reason is that this technique is one dimensional since it involves the variation of only a single time interval. They have further pointed out that multidimensional techniques in which independent control over several time intervals between short pulses is maintained provide a much more sensitive probe for the structure and dynamics of molecules in the condensed phase. Multidimensional techniques are commonly used in nuclear magnetic resonance spectroscopy[4] to provide invaluable information on the structure and dynamics of complex molecules.[5]

The basic multidimensional scheme involves the application of n pairs of short pulses which generate and manipulate vibrational coherence in the ground state, followed by a final detection pulse which is scattered off the sample. The signal field is then proportional to the incoming field to the $2n+1$th power and is related to the nonlinear susceptibility $\chi^{(2n+1)}$. Since n time intervals between pulses are controlled, the technique constitutes an n-dimensional spectroscopy. CARS is the lowest (third order, $n=1$) technique of this type. The first suggestion was to construct the Raman analogue of the photon echo which is a seventh-order technique with three independent time intervals ($n=3$).[3] Such measurements have been reported on high-frequency intramolecular vibrations in several liquids.[6,7] Tanimura and Mukamel have later showed how lower (fifth-) order ($n=2$) techniques may be used to probe the nature of the spectral density obtained in CARS measurements.[8] Numerous experimental[7,9–11] and theoretical[12–17] studies have subsequently focused on using this two-dimensional technique to probe intermolecular nuclear dynamics in liquids. The capacity of two-dimensional vibrational spectroscopy to study the couplings between specific molecular vibrations has been demonstrated recently.[11]

Although only ground electronic state dynamics is probed in electronically off-resonant spectroscopy, calculations of optical signals still constitute a complex task due to the anharmonicities and the quantum character of nuclear motions. An approach based on a perturbative expansion of the signals in powers of anharmonicities and nonlinearities of the effective dipole operator has been recently proposed[11,17] and applied to the interpretation of fifth-order two-dimensional experiments. However, the calculation of higher-order optical signals which carry more detailed information requires a rapidly growing number of anharmonicities and nonlinearities. A systematic procedure is needed for sorting out the main contributions and finding the corrections to the leading terms. The use of classical approximations is very appealing in that regard. To set the stage we consider a particle of mass M moving in the Morse potential $U(Q)$:[18]

$$U(Q)=D(e^{-2aQ}-2e^{-aQ}+1). \tag{1.1}$$

This potential has a minimum at $Q=0$, and we set $U(0)=0$. For sufficiently small values of $\hbar$ it has bound (discrete) levels with energies:[18]

$$\varepsilon_n=D-D\left[1-\frac{\hbar\Omega_0}{2D}\left(n+\frac{1}{2}\right)\right]^2, \quad \left(n+\frac{1}{2}\right)<\frac{2D}{\hbar\Omega_0}, \tag{1.2}$$

where $n=0,1,\ldots$ and $\Omega_0\equiv a(2D/M)^{1/2}$ is the harmonic frequency of the Morse potential. Although $\hbar$ has a well-defined value, semiclassical expansions can be conveniently performed by varying it as a parameter. According to the correspondence principle, eigenstates with a high quantum number $n\gg 1$ may be calculated semiclassically. Let us denote by n_T the quantum number of a state whose energy is

$\varepsilon_{n_T} \simeq kT$. The system will thus behave classically in the high temperature limit whereby $n_T \gg 1$. For the Morse potential this gives

$$kT \gg \frac{\hbar\Omega_0}{2}\left(2-\frac{\hbar\Omega_0}{2D}\right). \tag{1.3}$$

All molecular properties (including the optical response functions) can be calculated classically in this case.[19] A systematic procedure for computing quantum corrections is outlined in Ref. 21. Nuclear modes in liquids typically span a broad frequency range, including low frequency modes with $\hbar\Omega \ll kT$ as well as modes with $\hbar\Omega \gtrsim kT$. In liquid water for example the spectral density covers the $0-1000\ \mathrm{cm}^{-1}$ range.[12] The high-temperature approximation is therefore not generally applicable.

In this paper we develop a regular (and less obvious) semiclassical expansion of the optical response (SEOR) in powers of the Planck constant $\hbar$ which does not invoke the high-temperature approximation. The leading contribution in this expansion can be obtained by solving classical equations of motion, and is temperature independent; the temperature shows up only in higher-order terms.

The SEOR is based on the following observation: The optical response of a harmonic system is classical, even for $\hbar\Omega > kT$ where the system's motions and equilibrium density matrix are quantum mechanical. This suggests that a semiclassical expansion for the response may be possible for weak anharmonicities (rather than at high temperature). To see that, we consider a harmonic oscillator whose dipole operator is linear in the coordinate Q. Its optical response can be obtained by solving the classical equation of motion

$$\frac{d^2Q}{d\tau^2}+\Omega^2 Q=\mu\mathscr{E}(\tau), \tag{1.4}$$

with the initial conditions

$$Q(-\infty)=0; \quad \left|\frac{dQ}{d\tau}\right|_{\tau=-\infty}=0. \tag{1.5}$$

Here Ω is the oscillator frequency, μQ is the dipole, and $\mathscr{E}(\tau)$ is the driving field. Equation (1.4) yields in the frequency domain $Q(\omega)=\mu(\Omega^2-\omega^2)^{-1}\mathscr{E}(\omega)$. The optical response is in this case temperature independent and is strictly linear (i.e. all optical nonlinearities vanish identically). This implies that the linear optical response of a harmonic oscillator behaves classically for all values of $\hbar$ and T. Optical nonlinearities can be induced by adding anharmonicities to the potential or by including a nonlinear dependence of the dipole operator on nuclear coordinates $\alpha(Q)$. In either case, the simple classical picture of optical response no longer holds. Nevertheless, when anharmonicities are sufficiently weak, the leading contribution to the response may still be obtained by solving the classical equation of motion

$$M\frac{d^2Q}{d\tau^2}+\frac{\partial U(Q)}{\partial Q}=\frac{\partial\alpha(Q)}{\partial Q}\mathscr{E}(\tau), \tag{1.6}$$

with the initial condition given by Eq. (1.5). Systematic corrections may then be calculated semiclassically. To define precisely the domain of applicability of the SEOR, we note that any physically realistic potential is essentially harmonic in the immediate vicinity of its minimum ($Q=0$). For the Morse potential, Eq. (1.2) implies that the spectrum is almost harmonic $\varepsilon_n \approx \hbar\Omega_0(n+\frac{1}{2})$ provided

$$\frac{\hbar\Omega_0}{2D} \ll 1 \tag{1.7}$$

and n is not too large so that

$$\frac{\hbar\Omega_0}{2D}\left(n+\frac{1}{2}\right) \ll 1. \tag{1.8}$$

At finite temperatures the system is almost harmonic as long as this condition holds for states with energies $\varepsilon_n \approx kT$. This yields

$$\frac{kT}{2D} \ll 1. \tag{1.9}$$

The SEOR applies when both Eqs. (1.7) and (1.9) are satisfied. Note that in this case the classical approximation for the response holds when the temperature is sufficiently low (to reduce the effects of anharmonicities). This is counterintuitive since the system itself behaves classically only at high temperatures! In the SEOR we only require the *response* to be classical: This is a weaker requirement than assuming that the nuclear motions are classical; this is why the SEOR applies even when the high-temperature approximation is not valid.

The conditions given by Eqs. (1.7) and (1.9) can be obtained alternatively in the following way: A nuclear displacement Q belongs to the harmonic region if

$$|U(Q)-U_0(Q)| \ll U_0(Q), \tag{1.10}$$

where $U_0(Q) \equiv M\Omega_0^2 Q^2/2$ is the harmonic part of the potential. For the Morse potential, Eq. (1.10) amounts to $aQ \ll 1$. We now introduce the characteristic quantum displacement $Q_\hbar$ and a thermal displacement Q_T by the conditions

$$\hbar\Omega_0 = U_0(Q_\hbar); \quad kT = U_0(Q_T). \tag{1.11}$$

Requiring that both $Q_\hbar$ and Q_T belong to the harmonic region, i.e.

$$aQ_\hbar \ll 1, \quad aQ_T \ll 1, \tag{1.12}$$

and making use of Eqs. (1.11) yields Eqs. (1.7) and (1.9). This derivation explains why Eq. (1.7) does not contain the temperature, whereas Eq. (1.9) does not contain the Planck constant.

In the high-temperature limit the time evolution can be calculated using classical propagation of distributions, i.e. wave packets representing the density matrix in the Wigner representation.[20] This requires calculating classical trajectories and sampling the initial conditions according to the equilibrium distribution.[19] Higher-order corrections in $\hbar$ can be calculated by using the path-integral representation in Liouville space and expanding the path integrals in $Q_- \equiv Q_L - Q_R$ where Q_L and Q_R stand for trajectories representing evolution of the left (ket) and the right (bra) components of the density matrix.[21] Note that Eq. (1.3), which defines the high-temperature limit, is satisfied for sufficiently small values of $\hbar$. The semiclassical expansion can then be carried out for-

mally by simply setting $\hbar \to 0$. We can extend this procedure to the SEOR as well by introducing the thermal frequency

$$\omega_T \equiv \frac{kT}{\hbar}. \tag{1.13}$$

Equations (1.7) and (1.9) now adopt the form

$$\frac{\hbar \Omega_0}{2D} \ll 1, \quad \frac{\hbar \omega_T}{2D} \ll 1. \tag{1.14}$$

Equations. (1.3) and (1.14) are satisfied for small values of $\hbar$ and provide a formal definition of the high-temperature expansions and the SEOR respectively. In both cases we expand the response in powers of $\hbar$. The difference is that in the former case we hold T fixed whereas in the latter we hold ω_T fixed. This results in a very different bookkeeping and a different limit as $\hbar \to 0$ since ω_T contains a ''hidden'' $\hbar$ factor in its definition. Note that when Eq. (1.7) holds, Eq. (1.3), which defines the high-temperature limit, adopts a simple form

$$\Omega_0 \ll \omega_T. \tag{1.15}$$

This condition need not be satisfied in the SEOR which is determined by Eq. (1.14).

The paper is organized as follows: In Section II we introduce our model, which consists of a set of interacting anharmonic molecular oscillators coupled to a bath, and present correlation function expressions for the optical signals. In Section III we introduce a harmonic model for the bath and outline the SEOR for these correlation functions in powers of $\hbar$. In Section IV we evaluate the leading (classical) terms in the SEOR for the response functions $R^{(3)}$ and $R^{(5)}$. The calculation is performed diagrammatically by retaining only tree diagrams. In Section V we show how the leading terms in the response functions $R^{(2n+1)}$ to any order can be obtained by solving classical equations of motion. This procedure is then used in Appendices B and C to derive the classical expression for $R^{(7)}$. The temperature-dependent first-order correction in $\hbar$ to $R^{(3)}$ is calculated in Appendix D. Finally our results are summarized in Section VI.

II. CORRELATION FUNCTION EXPRESSIONS FOR THE SIGNAL FIELD

The Hamiltonian representing vibrational motions in the ground electronic state is given by the sum of the nuclear kinetic energy and the ground state adiabatic potential $U(\mathbf{Q})$ where Q_j are the nuclear coordinates. We choose the origin of $\mathbf{Q}$ at the minimum of $U(\mathbf{Q})$ which corresponds to the optimized molecular geometry, and represent the potential as a sum of the harmonic part (quadratic terms in $\mathbf{Q}$) and the anharmonic part $V(\mathbf{Q})$ (higher-order terms). By diagonalizing the harmonic potential, we can switch to the vibrational normal mode representation, and recast the molecular Hamiltonian H_m in the form

$$H_m = \sum_j \left(\frac{P_j^2}{2M_j} + \frac{M_j \Omega_j^2 Q_j^2}{2} \right) + V(\mathbf{Q}), \tag{2.1}$$

where $P_j(Q_j)$ is the momentum (coordinate) operator of the jth normal mode, Ω_j and M_j are its frequency and reduced mass respectively. Low-frequency intermolecular degrees of freedom $\mathbf{q}$ and their coupling to the intramolecular modes are described by the Hamiltonian H_B whose precise form need not be specified at this point. The material Hamiltonian is given by[22]

$$H = H_m(\mathbf{Q}) + H_B(\mathbf{Q}, \mathbf{q}). \tag{2.2}$$

If the driving optical field is off-resonant with respect to electronic transitions, and the ground state has no permanent dipole, the coupling of the vibrational degrees of freedom to the driving field $\mathscr{E}(\tau)$ can be described by the effective interaction Hamiltonian[3,8,23]

$$H_{int}(\tau) = -\mathscr{E}^2(\tau)\alpha(\mathbf{Q}), \tag{2.3}$$

where $\alpha(\mathbf{Q})$ is the electronic polarizability which acts as an operator in the vibrational space. The total Hamiltonian $H_T(\tau)$ (which includes the coupling to the driving field) is finally given by

$$H_T(\tau) = H + H_{int}(\tau). \tag{2.4}$$

The induced polarization $S(\tau)$ at time τ is given by the expectation value of the effective polarizability operator

$$S(\tau) = \mathscr{E}_s(\tau)\langle \tilde{\alpha}(\tau) \rangle, \tag{2.5}$$

where for any operator A, $\tilde{A}(\tau)$ denotes the Heisenberg operator whose time evolution is governed by $H_T(\tau)$. We represent the driving field as a sum of n nonoverlapping pulses centered at times $\tau_1, \ldots, \tau_n$; $\tau_1 < \tau_2 < \ldots < \tau_n$,

$$\mathscr{E}(\tau) = \sum_{p=1}^{n} \mathscr{E}_p(\tau - \tau_p). \tag{2.6}$$

In addition $\mathscr{E}_s(\tau - \tau_s)$ with $\tau_s > \tau_n$ is the final probe field which generates the signal according to Eq. (2.5). Equation (2.3) implies that the effective driving field $F(\tau)$ should be defined by

$$F(\tau) = \sum_{p=1}^{n} \mathscr{E}_p^2(\tau - \tau_p). \tag{2.7}$$

The optical polarization can be represented in a form

$$S(t) = \left\langle \alpha_+(t) \exp\left[\frac{i}{\hbar} \int_{-\infty}^{t} d\tau F(\tau) \alpha_-(\tau) \right] \right\rangle \mathscr{E}_s(t - t_s). \tag{2.8}$$

Here $\alpha_\pm$ are superoperators acting in Liouville space [Eq. (A3)], $\alpha(t)$ are interaction-picture operators whose time evolution is given by the material Hamiltonian H [Eq. (2.2)]. Equation (2.8) is a Liouville space correlation function which is a shorthand notation for a combination of ordinary (Hilbert space) correlation functions. By expanding the exponent in the right-hand side of Eq. (2.8) in powers of $F(\tau)$, and representing $F(\tau)$ in the form of Eq. (2.7) we obtain an expansion of the signal in powers of the incoming electric fields. The polarization (and the signal field) $S^{(2n+1)}$ in multidimensional vibrational spectroscopy performed with n pulses is proportional to the square of the field of each of the n driving pulses and to the probe field, and is altogether $(2n+1)$th order in the field. It is given by

$$S^{(2n+1)}(t)=\int_{-\infty}^{\infty}dt_1\ldots\int_{-\infty}^{\infty}dt_nR^{(2n+1)}(t;t_n,\ldots,t_1)\times\mathscr{E}_n^2(t_n-\tau_n)\ldots\mathscr{E}_1^2(t_1-\tau_1)\mathscr{E}_s(t-t_s), \quad (2.9)$$

with the response function

$$R^{(2n+1)}(t;\tau_n,\ldots,\tau_1)\equiv\left(\frac{i}{\hbar}\right)^n\langle\alpha_+(t)\alpha_-(\tau_n)\ldots\alpha_-(\tau_1)\rangle. \quad (2.10)$$

Equation (2.10) is an abbreviated notation for

$$R^{(2n+1)}(t;\tau_n,\ldots,\tau_1)=\left(\frac{i}{\hbar}\right)^n\langle[\ldots[[\alpha(t),\alpha(\tau_n)],\alpha(\tau_{n-1})]\ldots,\alpha(\tau_1)]\rangle. \quad (2.11)$$

In the impulsive limit, where the pulse durations are much shorter than the delay between pulses and the nuclear dynamics time scale, the time-resolved signal field assumes the form

$$S^{(2n+1)}=R^{(2n+1)}(t_s;\tau_n,\ldots,\tau_1)F_n\ldots F_1\overline{\mathscr{E}}_s, \quad (2.12)$$

where

$$F_j\equiv\int_{-\infty}^{\infty}d\tau\mathscr{E}_j^2(\tau), \quad \overline{E_s}\equiv\int_{-\infty}^{\infty}d\tau\mathscr{E}_s(\tau). \quad (2.13)$$

It should be emphasized that the time arguments in Eq. (2.12) are fully ordered $\tau_1\leqslant\tau_2\ldots\leqslant\tau_n\leqslant t_s$.

The observed signal depends on the mode of detection. Ordinary homodyne detection probes $|S^{(2n+1)}|^2$ integrated over t_s. Heterodyne techniques can be used to probe separately the real and the imaginary parts of $S^{(2n+1)}$ itself.[22] We shall therefore focus on the signal field $S^{(2n+1)}$ which carries the most detailed information about the system. In the next section we develop a semiclassical procedure for computing the signal field.

III. SEMICLASSICAL EXPANSION OF RESPONSE FUNCTIONS

In this section we develop a procedure for calculating the response function $R^{(2n+1)}$ (Eq. (2.10)). Semiclassical expansions are usually carried out in powers of $\hbar$ for a given temperature T. This results in the high-temperature limit $\Omega\ll\omega_T$ for $\hbar\to0$ (here Ω is a typical vibrational frequency).[19] In contrast, the SEOR is obtained by fixing the thermal frequency ω_T rather than T and then expanding the signal in powers of $\hbar$. The temperature should therefore be given by $T=k^{-1}\hbar\omega_T$.

To develop the SEOR we first note that if $V(\mathbf{Q})=0$ in Eq. (2.1) (i.e. the system is harmonic), the correlation function in Eq. (2.10) can be evaluated exactly;[22] the anharmonic terms $V(\mathbf{Q})$ can then be incorporated perturbatively. We shall show that only a finite number of terms in the expansion contribute to a given order in $\hbar$. Collecting all of these terms we obtain an expansion in $\hbar$. We first expand the anharmonic potential $V(\mathbf{Q})$ and the effective dipole operator α in powers of Q_j:

$$V(\mathbf{Q})=\sum_{N=3}^{\infty}\frac{1}{N!}V^{(N)}_{j_1\ldots j_N}Q_{j_1}\ldots Q_{j_N}, \quad (3.1)$$

$$\alpha=\sum_{N=1}^{\infty}\frac{1}{N!}\alpha^{(N)}_{j_1\ldots j_N}Q_{j_1}\ldots Q_{j_N}. \quad (3.2)$$

The Hamiltonian H can be partitioned as

$$H=H_0+V(\mathbf{Q}), \quad (3.3)$$

where

$$H_0\equiv\sum_j\left(\frac{P_j^2}{2M_j}+\frac{M_j\Omega_j^2Q_j^2}{2}\right)+H_B, \quad (3.4)$$

is its harmonic part. Equation (2.10) can be recast in the form

$$R^{(2n+1)}(t;\tau_n,\ldots,\tau_1)=\left(\frac{i}{\hbar}\right)^n\left\langle\alpha_+(t)\alpha_-(\tau_n)\ldots\alpha_-(\tau_1)\times\exp\left\{-\frac{i}{\hbar}\int_{-\infty}^{\tau_+}d\tau V_-[\mathbf{Q}(\tau)]\right\}\right\rangle_0. \quad (3.5)$$

Equation (3.5) constitutes the interaction-picture representation of the correlation function (Eq. (2.10)).[24,25] All Liouville space superoperators in this expression should be taken to be chronologically time ordered from right (early time) to left (late time). $\langle\ldots\rangle_0$ denotes the expectation value in the system with the Hamiltonian H_0, and τ_+ should satisfy the condition $\tau_+\geqslant t$.[24] In some cases it is convenient to set $\tau_+=t$, in other applications it is preferable to choose $\tau_+=+\infty$. Equation (3.5) is different from the three-part time contour used in Ref. 17. In Appendix A we show that in the presence of a bath both representations are equivalent.

The expansion of the signal in powers of $V^{(N)}$ and $\alpha^{(N)}$ is carried out in a standard way. We first expand the exponent in Eq. (3.5) in powers of $V(\mathbf{Q})$:

$$R^{(2n+1)}(t;\tau_n,\ldots\tau_1)=\sum_{m=0}^{\infty}\left(\frac{i}{\hbar}\right)^{m+n}(-1)^m\int_{-\infty}^{\tau_+}d\tau_1'\ldots\times\int_{-\infty}^{\tau_+}d\tau_m'\langle\alpha_+(t)\alpha_-(\tau_n)\ldots\alpha_-(\tau_1)\times V_-[\mathbf{Q}(\tau_m')]\ldots V_-[\mathbf{Q}(\tau_1')]\rangle_0. \quad (3.6)$$

By expanding $\alpha_+(t)$, $\alpha_-(\tau_j)$, and $V[\mathbf{Q}(\tau_j')]$ in a Taylor series in Q_{j+} and Q_{j-} and using Eqs. (3.1) and (3.2), we express the signal in terms of multipoint correlation functions $\langle Q_{j_1\nu_1}(\tau_1)\ldots Q_{j_N\nu_N}(\tau_N)\rangle_0$ where $\nu_{1,\ldots,}\nu_N=\pm$. At this point we need to specify the nature of the intermolecular bath degrees of freedom and their coupling to the vibrational modes. For the sake of simplicity we assume a harmonic bath linearly coupled to the intramolecular coordinates Q_j,

$$H_B=\sum_{j\alpha}\left[\frac{p_{j\alpha}^2}{2m_{j\alpha}}+\frac{m_{j\alpha}\omega_{j\alpha}^2}{2}\left(q_{j\alpha}-\frac{c_{j\alpha}}{m_{j\alpha}\omega_{j\alpha}}Q_j\right)^2\right], \quad (3.7)$$

where $p_{j\alpha}(q_{j\alpha})$ are momentum (coordinate) operators of bath oscillators. The applicability of this model and possible

extensions are discussed in Section VI. Using the Wick theorem, which holds for harmonic systems, the multipoint correlation functions can be factorized as products of two-point correlation functions

$$G_{ij}^{(-)}(\tau)\equiv\hbar^{-1}\langle Q_{i+}(\tau)Q_{j-}(0)\rangle_0,$$
and
$$G_{ij}^{(+)}(\tau)\equiv\hbar^{-1}\langle Q_{i+}(\tau)Q_{j+}(0)\rangle_0. \tag{3.8}$$

This factorization greatly simplifies the resulting nonlinear response functions, which makes it possible to gain useful physical insight. Note that $G_{ij}^{(\pm)}(\tau)$ do not depend on $\hbar$ since the expectation values $\langle Q_{i+}(\tau)Q_{j\pm}(0)\rangle$ are proportional to $\hbar$. These two-point correlation functions can be expressed in terms of the matrix of spectral densities $C_{ij}(\omega)$:[22,25]

$$\langle Q_{i+}(\tau)Q_{j-}(0)\rangle=2i\hbar\,\theta(\tau)\int_{-\infty}^{\infty}\frac{d\omega}{2\pi}C_{ij}(\omega)\sin(\omega\tau), \tag{3.9}$$

$$\langle Q_{i+}(\tau)Q_{j+}(0)\rangle=\hbar\int_{-\infty}^{\infty}\frac{d\omega}{2\pi}C_{ij}(\omega)\times\coth\left(\frac{\omega}{2\omega_T}\right)\cos(\omega\tau).$$

Each contribution to the signal can be conveniently represented by a diagram[26,27] where vertices denote the quantities $\alpha^{(m)}_{i_1\ldots i_m}$ and $V^{(m)}_{i_1\ldots i_m}$ whereas lines represent the two-point correlation functions given by Eqs. (3.8) and (3.9). Given $\alpha^{(m)}_{i_1\ldots i_m}$, $V^{(m)}_{i_1\ldots 1_m}$ and $C_{ij}(\omega)$ as an input, each contribution (diagram) can be calculated explicitly. The bookkeeping in these diagrams is different from that used in the double-sided Feynman diagrams:[22] In the present approach we keep track of interaction times with the driving field, and the various terms in the expansion of $\alpha(\mathbf{Q})$ [Eq. (3.2)] which participate in interactions. The double-sided Feynman diagrams maintain a much more detailed bookkeeping: Each diagram represents a Liouville space pathway with a well defined time ordering of the various interactions with the ket and the bra of the density matrix. Each of the present diagrams may represent many Liouville space pathways, resulting in a considerably more compact expression. To expand the signal in powers of $\hbar$ we introduce for each diagram the number of vertices N_0, lines N_1, and loops N_L. We also define the reduced Euler characteristic χ of a diagram,

$$\chi\equiv N_1-N_0+1. \tag{3.10}$$

It follows from Eqs. (3.6) and (3.9) that each diagram contains an $\hbar^{\chi}$ factor. For connected diagrams we have $\chi=N_L$. Since only connected diagrams contribute to the signal,[24] each diagram carries an $\hbar^{N_L}$ factor, which implies that the expansion in $\hbar$ is synonymous to an expansion in the number of loops N_L. An important consequence of this well-known result of field theory[28] is that only a finite number of diagrams contribute to $R^{(2n+1)}$ for a given N_L. Each contribution to a given order of $\hbar$ can therefore be evaluated explicitly, resulting in a regular expansion in $\hbar$. The Planck constant thus provides a convenient bookkeeping device that allows us to classify the numerous contributions in a unique and systematic way. The lowest contribution, represented by tree diagrams [i.e. with $N_L=0$], can be alternatively obtained by solving classical equations of motion, as will be demonstrated in the coming sections. Higher-order terms provide quantum corrections.

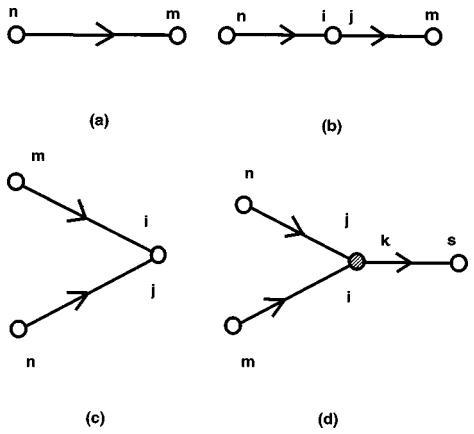

FIG. 1. Diagrammatic representation of $R^{(3)}$ and $R^{(5)}$. Arrows indicate forward propagation in time. Lines denote the retarded Green functions $G^{(-)}$, empty circles stand for $\alpha^{(N)}$ whereas filled circles denote $V^{(N)}$.

IV. OPTICAL RESPONSE-FUNCTIONS IN THE CLASSICAL LIMIT

In this section we derive expressions for $R^{(3)}$ and $R^{(5)}$ in the classical approximation. $R^{(3)}$ is given by a single term represented by the diagram with no vertices shown in Fig. 1(a). It can be obtained from Eq. (3.6) by using $n=1$, setting the exponent in the rhs of Eq. (3.6) to one, and retaining only the linear terms in the expansion of the polarizability operators α [Eq. (3.2)]. Making use of Eq. (3.9) finally yields:

$$R^{(3)}(t;\tau)=\sum_{mn}\alpha_m^{(1)}\alpha_n^{(1)}C_{mn}(t-\tau), \tag{4.1}$$

where $C_{mn}(t)$ is the spectral density in the time domain:

$$C_{mn}(t)=-2\,\theta(t)\int\frac{d\omega}{2\pi}C_{mn}(\omega)\sin(\omega t). \tag{4.2}$$

$R^{(5)}$ is similarly given by a sum of three contributions represented diagrammatically in Figs. 1(b)–1(d),

$$R^{(5)}(t;\tau_2,\tau_1)=\sum_{\alpha=1}^{3}R_{\alpha}^{(5)}(t;\tau_2,\tau_1). \tag{4.3}$$

The first two terms (Figs. 1(b) and 1(d)) are obtained by setting the exponent in Eq. (3.5) to one. For Fig. 1(b) we take the second-order term in the expansion [Eq. (3.2)] of $\alpha_-(\tau_2)$ and the first-order terms for $\alpha_+(t)$ and $\alpha_-(\tau_1)$,

$$R_1^{(5)}(t;\tau_2,\tau_1)\equiv\sum\alpha_{ij}^{(2)}\alpha_m^{(1)}\alpha_n^{(1)}C_{mj}(t-\tau_2)C_{in}(\tau_2-\tau_1). \tag{4.4}$$

In Eq. (4.4) and hereafter, a bare summation symbol with no indices implies the summation over repeating indices.

For Fig. 1(c) we take the second-order terms for $\alpha_+(t)$ and first-order terms for $\alpha_-(\tau_1),\alpha_-(\tau_2)$,

$$R_2^{(5)}(t;\tau_2,\tau_1)=\sum \alpha_{ij}^{(2)}\alpha_m^{(1)}\alpha_n^{(1)}C_{im}(t-\tau_2)C_{jn}(t-\tau_1). \tag{4.5}$$

The third contribution to $R^{(5)}$ is obtained by taking the first-order term in the expansion of the exponent in Eq. (3.5) in powers of V_-, the third-order term in the expansion of V_- in powers of Q_j [Eq. (3.1)] and the first-order terms in Q_j for $\alpha_+(t),\alpha_-(\tau_2)$ and $\alpha_-(\tau_1)$. This yields

$$R_3^{(5)}(t;\tau_2,\tau_1)=-\sum \int_{\tau_2}^{t} d\tau V_{ijk}^{(3)}\alpha_m^{(1)}\alpha_n^{(1)}\alpha_s^{(1)}C_{sk}(t-\tau) \times C_{im}(\tau-\tau_1)C_{jn}(\tau-\tau_2). \tag{4.6}$$

A closed expression for $R^{(7)}$ derived using the present classical level of theory is given in Appendix C. The quantum correction to $R^{(3)}$, to first-order in $\hbar$, is calculated in Appendix D. In the classical approximation all response functions are independent of temperature. In contrast, the quantum corrections to $R^{(3)}$ do depend on temperature. Consequently, even if these corrections are small compared to their classical counterparts, they can be probed experimentally by monitoring the variation of the signals with temperature.

V. CLASSICAL EQUATIONS OF MOTION FOR OPTICAL RESPONSE

In Section IV and in Appendix C we calculated the optical response functions $R^{(3)}$, $R^{(5)}$ and $R^{(7)}$ to zeroth order in $\hbar$ by keeping the leading term in the SEOR. In this section we show how these results can be obtained alternatively by solving classical equations of motion, expanded to the desired order in the driving field. The equation of motion procedure is most suitable for numerical simulations. It further clarifies the nature of the approximations involved in the SEOR and can be readily applied for calculating higher-order response functions $R^{(2n+1)}$. In the next section we outline how this procedure may be modified to incorporate quantum corrections to higher order in $\hbar$. Equations of motion based on the time dependent Hartree–Fock (TDHF) procedure provide the standard tool for the calculation of optical nonlinearities of semiconductors (the semiconductor Bloch equations)[29] and conjugated molecules.[30] Conceptually the present equations share many formal similarities with the TDHF: In both cases we consider a quantum system whose optical response may nevertheless be calculated using classical equations of motion. In the TDHF the dynamical variables are the elements of the reduced single electron density matrix whereas in the present application they are the nuclear displacements.

We consider the classical limit of the anharmonic system given by Eqs. (3.1)–(3.4) by first neglecting the bath ($H_B=0$). The system driven by the effective external field $F(\tau)$ is described by a classical Hamiltonian

$$H=\sum_j \left(\frac{P_j^2}{2M_j}+\frac{M_j\Omega_j^2Q_j^2}{2}\right)+V(\mathbf{Q})-F(\tau)\alpha(Q), \tag{5.1}$$

with the standard Poisson bracket

$$\{P_i,Q_j\}=\delta_{ij}. \tag{5.2}$$

The classical equations of motion can be represented in the form

$$\frac{dP_i}{d\tau}=\{H,P_i\},\quad \frac{dQ_i}{d\tau}=\{H,Q_i\}. \tag{5.3}$$

Equations (5.1)–(5.3) yield

$$\frac{dQ_j}{d\tau}=\frac{P_j}{M_j},\qquad \frac{dP_j}{d\tau}=-M_j\Omega_j^2Q_j-\frac{\partial V(\mathbf{Q})}{\partial Q_j}+F(\tau)\frac{\partial\alpha(\mathbf{Q})}{\partial Q_j}. \tag{5.4}$$

Using these equations, the polarization (and the classical response) is given by

$$\alpha(\tau)=\alpha(\mathbf{Q}(\tau)), \tag{5.5}$$

where $\mathbf{Q}(\tau)$ evolve using classical trajectories

$$M_j\frac{d^2Q_j}{d\tau^2}+M_j\Omega_j^2Q_j=-\frac{\partial V(\mathbf{Q})}{\partial Q_j}+F(\tau)\frac{\partial\alpha(\mathbf{Q})}{\partial Q_j}, \tag{5.6}$$

with the initial conditions

$$Q_j(-\infty)=0\quad \left.\frac{dQ_j}{d\tau}\right|_{\tau=-\infty}=0. \tag{5.7}$$

Note that Eq. (5.7) represents a stationary point of Eq. (5.6) when the external field is switched off.

Equations (5.5)–(5.7) provide a simple algorithm for computing the optical response in the classical limit. The response functions $R^{(2n+1)}$ are obtained by expanding the solution of Eq. (5.6) in powers of the driving field. The contributions to the response functions can be represented by tree diagrams similar to those used in Section IV and in Appendix C. The only difference is that we need to substitute the Green function on the lhs of Eq. (5.6) for the Green function $G_{ij}^{(-)}(\tau)$ defined by Eq. (3.8). In the absence of a bath the two coincide. To incorporate the bath, the lhs of Eq. (5.6) should be modified so that the Green function of the equation reproduces $G_{ij}^{(-)}(\tau)$ with a bath given by Eqs. (3.8) and (3.9). This can be easily accomplished by adding a matrix of memory functions $\gamma_{ij}(\tau)$. Equation (5.6) then becomes

$$M_j\frac{d^2Q_j}{d\tau^2}+M_j\Omega_j^2Q_j+\sum_i \int_{-\infty}^{\tau} d\tau'\,\gamma_{ji}(\tau-\tau')Q_i(\tau') =-\frac{\partial V(\mathbf{Q})}{\partial Q_j}+F(\tau)\frac{\partial\alpha(\mathbf{Q})}{\partial Q_j}, \tag{5.8}$$

where $\gamma_{ij}(\tau-\tau')$ is the retarded Green function of collective bath coordinates coupled to primary coordinates Q_i and Q_j. It follows from causality that this Green function vanishes for $\tau<\tau'$. It can be expressed in terms of $C_{ij}(\omega)$ by comparing the ''linear'' response function $R^{(3)}$ obtained using Eqs. (5.5), (5.8), and (5.7) with Eqs. (4.1) and (4.2). This can be easily accomplished by solving Eq. (5.8) and switching to the frequency domain, which yields:

$$C_{mn}(\omega)=\mathrm{Im}\{[h(\omega)^{-1}]_{mn}\}, \tag{5.9}$$

where

$$h_{mn}(\omega)\equiv\delta_{mn}M_n(\Omega_n^2-\omega^2)+\gamma_{mn}(\omega), \tag{5.10}$$

and the matrix $\gamma_{mn}(\omega)$ is the Fourier transform of the memory function:

$$\gamma_{mn}(\omega)\equiv\int_{-\infty}^{\infty}d\tau e^{i\omega\tau}\gamma_{mn}(\tau). \tag{5.11}$$

(Note that the lower integration limit may be changed to 0 since $\gamma(\tau)$ vanishes for $\tau<0$.)

Equations (5.5), (5.8), and (5.7) constitute a closed system of equations for the optical response of the system coupled to a harmonic bath to zero order in $\hbar$ within the SEOR. These equations can be used to calculate $R^{(2n+1)}$ to any order. For $R^{(3)}$ and $R^{(5)}$, they reproduce the results of Section IV. Closed expressions for $R^{(7)}$ obtained using the equations of motion approach are presented in Appendix C.

VI. DISCUSSION

In this paper we have explored the signatures of weak anharmonicities and nonlinearities in the expansion of the electronic polarizabilities in intramolecular coordinates in multidimensional nuclear spectroscopies. These techniques should be most valuable in the studies of unresolved vibrational bands that occur in liquids as well as complex molecules.[31] Protein nuclear dynamics for example spans a broad range of timescales ranging from femtosecond high frequency vibrations to seconds (protein folding).[32–34] Multidimensional spectroscopy could develop into an interesting new window for molecular structure and dynamics.

Adopting a simple harmonic model for intermolecular motions allowed us to derive analytical expressions for optical response functions and analyze the role of anharmonicities and dipole nonlinearities. In a realistic liquid intermolecular motions are anharmonic and the Wick theorem used in Section III to derive expressions for the optical response functions no longer holds. A more microscopic description which properly takes into account the intermolecular force field requires the development of numerical techniques for the direct simulation of the necessary multipoint correlation functions (Eq. (3.6)). This can be done e.g. using classical simulations.[20] It is important to note that the bath anharmonicities provide an additional source of optical nonlinearities. However, although intermolecular motions may be strongly anharmonic, their contribution to optical nonlinearities can be considerably reduced because of the collective nature of their coupling to intramolecular motions. Anharmonicities of the bath should also affect our predictions of temperature dependencies since the bath-induced optical nonlinearities are temperature dependent even to lowest order in intramolecular anharmonicities. Exploring the relative magnitudes of the intramolecular and bath contributions to the signal and its temperature dependence should be an interesting goal of numerical simulations.

Using the harmonic bath model we developed a semiclassical theory for multidimensional Raman spectroscopy of weakly anharmonic vibrations. Semiclassical approximations ordinarily hold when the temperature is high compared to all relevant vibrational frequencies. The present SEOR points to a much less obvious, low-temperature weak anharmonicity regime, where the optical response of the system behaves almost classically even though its equilibrium state may be in the quantum regime. We have shown that a semiclassical expansion of the response in $\hbar$ is possible even when the temperature is low compared with the vibrational frequencies, and the system is highly quantum. The leading terms in the expansion can be obtained by solving classical equations of motion. A systematic procedure for calculating quantum corrections to response functions was formulated and applied to derive the first-order quantum correction to $R^{(3)}$.

The motivation for performing a semiclassical expansion in the weak anharmonicity regime has been outlined in Section I using arguments based on the quantum states of the system. Below we present an alternative physical picture based on the evolution of nuclear wave packets, and show how quantum corrections can be obtained by solving coupled classical equations of motion which include higher-order dynamical variables.[35]

The state of the system at time τ is determined by the Liouville space wave packet $\rho(\mathbf{Q}_L,\mathbf{O}_R;\tau)$ which represents the system's density matrix in the nuclear space, where $\mathbf{Q}$ denotes the complete set of nuclear coordinates. The wave packet can be also represented using the Wigner phase-space representation

$$\rho_W(\mathbf{P},\mathbf{Q})\equiv\int d\mathbf{Q}_- e^{i\mathbf{P}\mathbf{Q}_-}\rho\left(\mathbf{Q}+\frac{\mathbf{Q}_-}{2},\mathbf{Q}-\frac{\mathbf{Q}_-}{2}\right). \tag{6.1}$$

It has been pointed out in Section I that semiclassical expansions are applicable in two regimes: the high-temperature and the weak anharmonicity limits. In the former case, the size of the equilibrium wave packet $\overline{\rho}(\mathbf{Q}_L,\mathbf{Q}_R)$ as a function of $\mathbf{Q}_-\equiv\mathbf{Q}_L-\mathbf{Q}_R$ for a fixed $\mathbf{Q}_+\equiv(\mathbf{Q}_L+\mathbf{Q}_R)/2$ is given by $Q_T^{(-)}$ defined by

$$Q_T^{(-)}\equiv(2MkT)^{-1/2}. \tag{6.2}$$

$Q_T^{(-)}$ is small at high temperatures. Assuming that the wave packet size along Q_- remains small even when the system is driven by the external field, the distribution of the momentum $\mathbf{P}$ which is conjugate to $\mathbf{Q}_-$ in the Wigner representation is broad, and the wave packet dynamics may be described by the classical Liouville equation; the propagation of the wave packet is thus determined by classical trajectories. Quantum corrections to the classical dynamics can be obtained by expanding the distribution in Q_- whose width is $\sim Q_T^{(-)}$, e.g. using the path-integral approach.[21] This implies that in the high-temperature limit the evolution is essentially classical because of the small wave packet size in the Q_- direction, compared to the length scale on which the potential varies.

To rationalize the semiclassical approach in the weak anharmonicity limit we start with a harmonic oscillator whose polarization operator is linear in the oscillator coordinates. The equilibrium wave packet is Gaussian; its size is determined by two length scales: the quantum-mechanical ($Q_\hbar$) and the temperature-induced (Q_T) contributions given by Eq. (1.11). The evolution induced by the driving field does not affect the shape of the wave packet and merely

changes its average position. Equation (1.4) can be interpreted as the equation for the dynamics of the wave packet position (i.e. the first moment of the wave packet). Stated differently, the position of the Liouville-space wave packet in the Wigner representation is given by (P,Q) and the phase-space dynamics of (P,Q) is given by Eq. (1.4) together with the definition

$$P = M\frac{dQ}{d\tau}. \tag{6.3}$$

This picture in particular clarifies the significance of the initial conditions [Eq. (1.5)]: They do not imply that the system is at a point in phase space but rather that the equilibrium wave packet is centered at $P=0$, $Q=0$.

When anharmonicities and dipole nonlinearities are taken into account, the wave packets are no longer Gaussian. Nevertheless, if these effects are small, one can expect weak deviations from the Gaussian form, which suggests that an expansion in these deviations is possible. Since the wave packet size is determined by $Q_\hbar$ and Q_T, the conditions of weak anharmonicity are given by Eq. (1.10) with $Q=Q_T,Q_\hbar$ which yields Eq. (1.14) for the Morse potential. The condition of weak nonlinearity in the expansion of the polarization operator [Eq. (3.2)] can be obtained by partitioning the polarization in Eq. (3.2) into the linear α^L and nonlinear α^{NL} parts corresponding to the $N=1$ and the $N>1$ terms in Eq. (3.2), and requiring

$$\frac{\partial\alpha^{NL}(Q)}{\partial Q} \ll \frac{\partial\alpha^L}{\partial Q}, \tag{6.4}$$

for $Q=Q_\hbar,Q_T$. This implies that the weak anharmonicity expansion is justified provided Eqs. (1.10) and (6.4) hold for $Q=Q_\hbar,Q_T$. Since as explained in Section I we fix ω_T (Eq. (1.13)), Eq. (1.11) implies $Q_T,Q_\hbar \sim \hbar^{1/2}$ and Eqs. (1.10) and (6.4) hold for small $\hbar$. This illustrates why the expansion in weak anharmonicities and polarization nonlinearities can be formally represented as an expansion in $\hbar$.

These arguments further suggest an alternative derivation of Eqs. (5.5), (5.8) and (5.7): We start with the Heisenberg equations of motion for the operators Q_j. Taking the expectation values of the Heisenberg equations and adopting the following factorization

$$\langle Q_{j_1}(\tau)\ldots Q_{j_n}(\tau)\rangle = \langle Q_{j_1}(\tau)\rangle\ldots\langle Q_{j_n}(\tau)\rangle, \tag{6.5}$$

yields Eq. (5.8). Equation (5.5) is obtained by applying Eq. (6.5) to the expectation value of Eq. (3.2) and Eq. (5.7) is obtained by neglecting the effects of anharmonicities in the equilibrium wave packet. This implies that the system of equations for the optical response derived in Section V using the Heisenberg equations of motion for nuclear coordinates is based on the truncation (Eq. (6.5)) which holds to zeroth order in $\hbar$. This may be illustrated by defining irreducible expectation values, for example

$$\langle\langle Q_iQ_j\rangle\rangle \equiv \langle Q_iQ_j\rangle - \langle Q_i\rangle\langle Q_j\rangle, \tag{6.6}$$

since $\langle\langle Q_iQ_j\rangle\rangle$ is proportional to the square of the wave packet size we obtain $\langle\langle Q_iQ_j\rangle\rangle\sim\hbar$ so that Eq. (6.5) holds to zero order in $\hbar$.

Quantum corrections to the response were calculated in Appendix D using diagrammatic techniques. The above arguments suggest a new approach for calculating these corrections. We start with the Heisenberg equations of motion for the expectation values $\langle Q_{j_1}(\tau)\ldots Q_{j_n}(\tau)\rangle$ for $n=1,\ldots,m$. These equations are closed using the following truncation scheme: We expand $\langle Q^s\rangle$ in lower-order irreducible expectation values $\langle\langle Q^j\rangle\rangle$, $j\leqslant s$, making use of the fact that the expansion of $\langle\langle Q^j\rangle\rangle$ starts at $\hbar^{j-1}$. Solving the closed system of equations perturbatively in $\hbar$ should result in a systematic expansion of the response functions. A similar procedure that includes bilinear combinations of coordinates and momenta has been introduced in Ref. 35.

As has been pointed out earlier, the classical level of theory closely resembles the calculation of the optical response of semiconductors and conjugated molecules using the semiconductor Bloch equations (SBE) or the time-dependent Hartree–Fock (TDHF) equations. We can use this analogy to show how $R^{(7)}$ measurements can be used to distinguish between contributions of anharmonicities and dipole nonlinearities. We first note that the response functions $R^{(2n+1)}$ are formally analogous to the nonlinear susceptibilities $\chi^{(n)}$ in electronically resonant measurements since both response functions depend on n time intervals between pulses. Upon replacing the effective electronic polarizability $\alpha(\mathbf{Q})$ by the dipole operator and the effective driving field $F(\tau)$ (Eq. 2.13) by the actual field, the formal expression for $R^{(2n+1)}$ turns into that of $\chi^{(n)}$. $R^{(3)}$ is thus analogous to $\chi^{(1)}$ and measures the linear nuclear response. Similarly $R^{(7)}$ and $\chi^{(3)}$ both depend on three time intervals. The expression for the polarization and the initial conditions obtained using the TDHF equations written in the eigenmode representation,[36] have exactly the same form as Eqs. (5.5), (5.6), and (5.7), despite their very different physical origin. We can use this analogy to predict effects for nuclear spectroscopy of liquids using the experience gained through the electronic spectroscopy of molecular aggregates and semiconductor nanostructures. Resonant time-domain phase-locked four-wave mixing techniques have the capacity to distinguish clearly between effects of non-Boson statistics(phase space filling) and electronic correlations in semiconductors.[29] These two types of nonlinearities are completely analogous to the dipole nonlinearities and anharmonicities respectively, in off-resonant Raman techniques. The reason for this capacity is the different way in which both types of nonlinearities enter the equations of motion [Eqs. (5.5) and (5.8)]: The polarization (or its analogue: phase space filling) is always multiplied by the field whereas the anharmonicity (or its analogue, electron correlations) is a purely material nonlinearity. The former creates interstate coherence impulsively upon acting with the field whereas in the latter, such coherence is created during the evolution periods between successive interactions with the fields.

The resonant photon-echo technique has been considered in Ref. 37 where the signal is observed in the direction $\mathbf{k}=\mathbf{2k}_2-\mathbf{k}_1$ and the pulses are short compared to the relaxation times and long compared to Ω^{-1}, Ω being the electronic transition frequency. The analogous technique in vibrational spectroscopy goes as follows: Let us assume that

each pulse is made out of a pair of overlapping pulses with wave vectors $\mathbf{k}',\mathbf{k}''$ and carrier frequencies ω',ω''; the pulses should be short compared to the relaxation time scale but long compared to Ω_j (Ω_j are the coherent vibrational frequencies). The effective field F then has the wave vector $\mathbf{k}''-\mathbf{k}'$ and the carrier frequency $\omega''-\omega'$. $\omega''-\omega'$ should be resonant with vibronic frequencies and the $R^{(7)}$ signal is observed in the direction

$$\mathbf{k}=2(\mathbf{k}_2''-\mathbf{k}_2')-(\mathbf{k}_1''-\mathbf{k}_1')+\mathbf{k}_s. \tag{6.7}$$

The last term in Eq. (6.7) originates from the pulse $\mathscr{E}_s$ [Eq. (2.5)]. In Ref. 37 it has been demonstrated how the phase of the photon-echo signal field may be used to distinguish between phase space filling and electron correlation types of nonlinearities. The same argument applied to the present technique suggests that the phase of the signal field (Eq. (6.7)) may be used to distinguish between effects of polarization nonlinearities and nuclear anharmonicities. This measurement requires a phase-sensitive detection which provides the joint time and frequency distribution (spectrogram) of the signal field.

ACKNOWLEDGMENTS

We gratefully acknowledge the support of the National Science Foundation and the United States Air Force Office of Scientific Research.

APPENDIX A: PERTURBATION THEORY FOR CORRELATION FUNCTIONS

In this Appendix we sketch the derivation of a perturbative expansion of correlation functions representing the optical response functions $R^{(2n+1)}$. The expansion is based on the Keldysh nonequilibrium perturbative technique[27] which has been applied earlier to the calculation of optical response functions.[24]

The formal expression for optical response functions in terms of the Liouville space correlation functions of the harmonic system is given by

$$\begin{aligned} R^{(2n+1)}(t;\tau_n,\ldots,\tau_1) &= \left\langle \alpha_+(t)\alpha_-(\tau_n)\ldots\alpha_-(\tau_1)\exp\left[-\frac{i}{\hbar}\int_{-\infty}^{\tau_+}d\tau V_-(\tau)\right]\right\rangle_0 \\ &\equiv \int dq_L dq_R \rho_0(q_L,q_R)\int_{M(q_L,q_R;\tau_+)}\mathscr{D}[Q(\tau)] \\ &\quad\times\exp\{iS_-^{(0)}[Q(\tau)]\}\alpha_+(t)\alpha_-(\tau_n)\ldots\alpha_-(\tau_1)\exp\left[-\frac{i}{\hbar}\int_{-\infty}^{\tau_+}d\tau V_-(\tau)\right]. \end{aligned} \tag{A1}$$

The path integration in Eq. (A1) is performed over the path space $M(q_L,q_R,\tau_+)$ of trajectories in Liouville space, i.e. $Q(\tau)\equiv(Q_L(\tau),Q_R(\tau))$ defined for $-\infty<\tau<\tau_+$ with the boundary conditions

$$\begin{aligned} &Q_L(-\infty)=q_L, \quad Q_R(-\infty)=q_R, \\ &Q_L(\tau_+)=Q_R(\tau_+). \end{aligned} \tag{A2}$$

For any operator $A(Q)$ we define

$$A_-\equiv A_L-A_R; \quad A_+\equiv\tfrac{1}{2}(A_L+A_R), \tag{A3}$$

$$A_L(Q)\equiv A(Q_L); \quad A_R(Q)\equiv A(Q_R). \tag{A4}$$

$S^{(0)}$ is the harmonic part of the action corresponding to the Hamiltonian H_0. The precise value of the time τ_+ is immaterial, as long as it satisfies the condition $\tau_+\geqslant t$. For the Keldysh technique[27] $\tau_+=+\infty$. In some applications it is more convenient to choose $\tau_+=t$.

At first glance it may seem that the equilibrium density matrix $\rho(q_L,q_R)$ of the system with anharmonicities included should be used in Eq. (A1) instead of its harmonic counterpart $\rho_0(q_L,q_R)$. However, for systems coupled to a bath, the result should be independent of the choice of the initial density matrix. Equation (A1) can be interpreted in the following way: We start with some initial distribution $\rho'(q_L,q_R)$ and a harmonic system at $\tau=-\infty$. The anharmonic interaction is then switched on adiabatically and (due to the system-bath coupling) the system reaches the new equilibrium state $\rho(q_L,q_R)$ of the interacting system. Consequently, the expectation values in Eq. (A1) are calculated with respect to the correct equilibrium state. The perturbative series is obtained by expanding the exponent in Eq. (A1) and applying the Wick theorem, as explained in Section III. This leads to a convenient diagrammatic technique which is a straightforward extension of the Keldysh technique; (corresponding to the choice $\tau_+=+\infty$). We will not repeat the rules of the diagrammatic technique, since they are given in standard textbooks (see e.g. Refs. 26 and 27).

We have shown that the perturbation theory can be formulated in a way that completely avoids the imaginary time loop used in Ref. 17. In the present formulation, the role of

this imaginary-time loop is played by the part of the Keldysh time loop which corresponds to $\tau<0$. However, to establish a connection between the two formalisms we will derive Eq. (A1) starting with the imaginary time loop. To that end we substitute $\rho(q_L,q_R)\equiv\langle q_R|\exp(-\beta H)|q_L\rangle$ with $\beta\equiv(kT)^{-1}$ for $\rho_0(q_L,q_R)\equiv\langle q_R|\exp(-\beta H_0)|q_L\rangle$ into Eq. (A1) and apply an imaginary-time path-integral representation for $\rho(q_L,q_R)$, which results in

$$R^{(2n+1)}(t;\tau_n,\ldots,\tau_1)=Z^{-1}\int dq_L dq_R\int_{M(q_L,q_R,\tau_+)}\mathscr{D}[Q(\tau)]\int_{M'(q_L,q_R;\beta)}\mathscr{D}[\bar{Q}(\tau')]$$
$$\times\exp\{iS_-^{(0)}[Q(\tau)]\}\exp\{-S_M^{(0)}[\bar{Q}(\tau')]\}\alpha_+(t)\alpha_-(\tau_n)\ldots\alpha_-(\tau_1)\exp\left[-\frac{i}{\hbar}\int_{-\infty}^{\tau_+}d\tau V_-(\tau)\right]$$
$$\times\exp\left[-\int_0^\beta d\tau' V(\tau')\right], \tag{A5}$$

with

$$Z\equiv\int dq\int_{M'(q,q,\beta)}\mathscr{D}[\bar{Q}(\tau')]\exp\{-S_M^{(0)}[\bar{Q}(\tau')]\}$$
$$\times\exp\left[-\int_0^\beta d\tau' V(\tau')\right]. \tag{A6}$$

Here $M'(q_L,q_R;\beta)$ denotes the space of trajectories $\bar{Q}(\tau')$ with $\tau'\in[0,\beta]$ and boundary conditions $\bar{Q}(0)=q_L$, $\bar{Q}(\beta)=q_R$; $S_M^{(0)}[\bar{Q}(\tau)]$ is the harmonic part of the imaginary-time Matsubara action.

The representation of Eqs. (A5) and (A6) corresponds to a time contour similar to the one used in Ref. 17. The difference is that the Matsubara loop is located at $\tau=-\infty$ rather than at $\tau=0$ (see Fig. 2). This leads to a similar perturbative expansion, however, the location of the Matsubara loop at $\tau=-\infty$ makes a substantial difference and leads to the representation of Eq. (A1). Expanding the last two exponents in Eq. (A5), we obtain two types of vertices induced by $V_-(\tau)$ and $V(\tau')$, hereafter referred to as Keldysh and Matsubara vertices respectively. We first note that only connected diagrams contribute to $R^{(2n+1)}$. Disconnected parts containing Matsubara vertices only do not contribute since they are cancelled by corrections to the partition function Z obtained by expanding Eq. (A6).[26] In the absence of such disconnected parts, and when a diagram is still not connected, there is a disconnected part which contains at least one ''minus'' operator, and no ''plus'' operator and the diagram vanishes.[24,25] If a diagram is connected and contains a Matsubara vertex it necessarily contains a Green function (a line) with an infinite difference of times; such a Green function vanishes if the system is coupled to a bath. This proves that only those diagrams which do not contain Matsubara vertices contribute to $R^{(2n+2)}$; these are precisely the diagrams obtained from the expansion of Eq. (A1). In summary, we have rederived our formalism based on the representation given by Eq. (A1) starting with the imaginary time loop formalism.

An alternative, more direct, although more tedious proof of the equivalence of these two formalisms, goes as follows: For any imaginary time loop diagram we switch to the frequency domain by using a continuous Fourier transform on the Keldysh part of the contour and a discrete Fourier transform on the Matsubara loop. Transforming sums over discrete frequencies to integrals over frequencies using the Gorkov–Eliashberg procedure[26] we can switch back to the time domain and obtain the contribution of the Keldysh diagram.

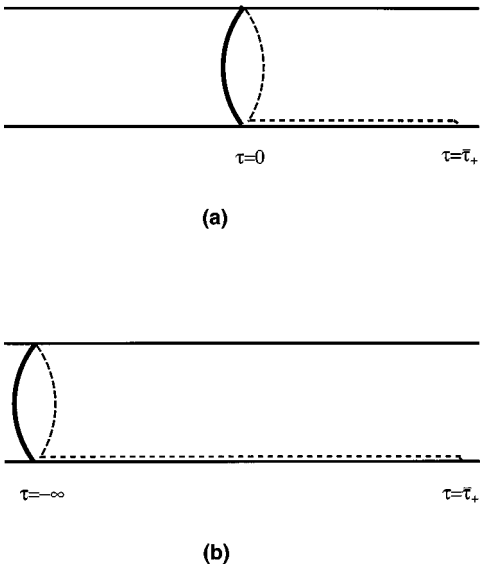

FIG. 2. Time contours used in Ref. 24 (a) and in Appendix A (b). Both contours are closed on the cylinder obtained from the complex plane by identifying $\tau+i\beta=\tau$ with $\beta=(kT)^{-1}$.

APPENDIX B: THE SEVENTH-ORDER OPTICAL RESPONSE FUNCTION

$R^{(7)}$ can be obtained by calculating perturbative terms represented by tree diagrams, as was done in Section IV for $R^{(3)}$ and $R^{(5)}$. Below we present a more intuitive derivation based on the classical equation of motion derived in Section V [Eq. (5.8)].

We start by expanding the polarization $\alpha(\tau)$ and the solution $Q(\tau)$ of Eq. (5.8) with the initial condition given by Eq. (5.7) in powers of the effective driving field $F(\tau)$:

$$\alpha(\tau)=\alpha^{(1)}(\tau)+\alpha^{(2)}(\tau)+\ldots, \tag{B1}$$

$$Q(\tau)=Q^{(1)}(\tau)+Q^{(2)}(\tau)+\ldots. \tag{B2}$$

Substituting Eqs. (B1) and (B2) into Eq. (5.5) and making use of the expansion of Eq. (3.2) we obtain

$$\alpha^{(1)}(\tau)=\sum_j \alpha_j^{(1)}Q_j^{(1)}(\tau), \tag{B3}$$

$$\alpha^{(2)}(\tau)=\sum_j \alpha_j^{(1)}Q_j^{(2)}(\tau)+\frac{1}{2}\sum_{ij}\alpha_{ij}^{(2)}Q_i^{(1)}(\tau)Q_j^{(1)}(\tau), \tag{B4}$$

$$\alpha^{(3)}(\tau)=\sum_j \alpha_j^{(1)}Q_j^{(3)}(\tau)+\sum_{ij}\alpha_{ij}^{(2)}Q_i^{(1)}(\tau)Q_j^{(2)}(\tau)+\frac{1}{6}\sum_{ijk}\alpha_{ijk}^{(3)}Q_i^{(1)}(\tau)Q_j^{(1)}(\tau)Q_k^{(1)}(\tau). \tag{B5}$$

When the expansion of Eq. (B2) is substituted into the equation of motion [Eq. (5.8)] we obtain

$$Q_i^{(1)}(\tau)=\sum_j \int_{-\infty}^{\tau} d\tau_1 C_{ij}(\tau-\tau_1)\alpha_j^{(1)}F(\tau_1), \tag{B6}$$

$$Q_i^{(2)}(\tau)=-\frac{1}{2}\sum_{mnj}V_{mnj}^{(3)}\int_{-\infty}^{\tau}d\tau_2 C_{ij}(\tau-\tau_2)Q_m^{(1)}(\tau_2)Q_n^{(1)}(\tau_2)+\sum_{mj}\alpha_{mj}^{(2)}\int_{-\infty}^{\tau}d\tau_2 C_{ij}(\tau-\tau_2)Q_m^{(1)}(\tau_2)F(\tau_2), \tag{B7}$$

$$\begin{aligned}Q_i^{(3)}(\tau)=&-\sum_{mnj}V_{mnj}^{(3)}\int_{-\infty}^{\tau}d\tau_3 C_{ij}(\tau-\tau_3)Q_m^{(1)}(\tau_3)\\&\times Q_n^{(2)}(\tau_3)-\frac{1}{6}\sum_{mnkj}V_{mnkj}^{(4)}\int_{-\infty}^{\tau}d\tau_3 C_{ij}(\tau-\tau_3)\\&\times Q_m^{(1)}(\tau_3)Q_n^{(1)}(\tau_3)Q_k^{(1)}(\tau_3)\\&+\sum_{mj}\alpha_{mj}^{(2)}\int_{-\infty}^{\tau}d\tau_3 C_{ij}(\tau-\tau_3)Q_m^{(2)}(\tau_3)F(\tau_3)\\&+\frac{1}{2}\sum_{mnj}\alpha_{mnj}^{(3)}\int_{-\infty}^{\tau}d\tau_3 C_{ij}(\tau-\tau_3)Q_m^{(1)}(\tau_3)\\&\times Q_n^{(1)}(\tau_3)F(\tau_3),\end{aligned} \tag{B8}$$

where $C_{ij}(\tau)$ is the Green function of the lhs of Eq. (5.8).

Substituting Eq. (B6) into Eq. (B3) yields the third-order response $R^{(3)}$ in the form of Eq. (4.1). This implies that $C_{ij}(\tau)$ defined in this appendix as the Green function of Eq. (5.8) coincides with that defined by Eq. (4.2) in terms of spectral densities. This is the reason for using the same notation. It then follows that $C_{ij}(\tau)$ in Eqs. (B6)–(B8) is given by Eq. (4.2).

To obtain $R^{(5)}$ we substitute Eq. (B6) into Eq. (B7) and then substitute Eqs. (B6) and (B7) into Eq. (B4). Making use of the definition of response functions [Eq. (2.9)] we obtain $R^{(5)}$ in the form of Eqs. (4.3)–(4.6).

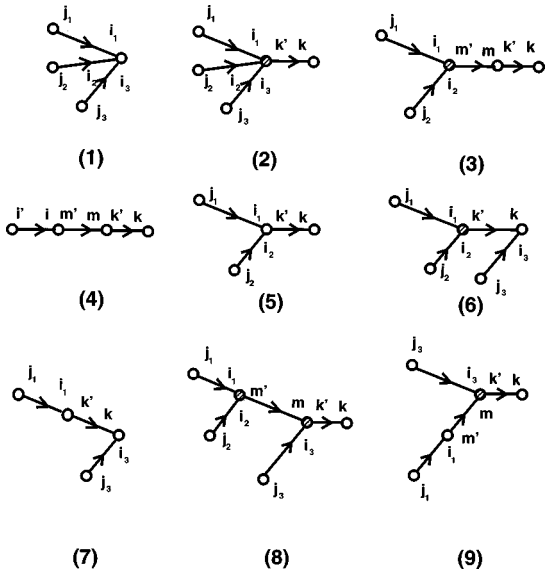

FIG. 3. The nine contributions to $R^{(7)}$ in the classical limit.

To calculate $R^{(7)}$ we first substitute Eq. (B6) into Eq. (B7) and then Eqs. (B6) and (B7) into Eq. (B8). This yields $Q^{(2)}$ in a form of a sum of two terms and $Q^{(3)}$ as a sum of six terms. The signal is obtained by substituting Eqs. (B6)–(B8) into Eq. (B5). The first term on the lhs of Eq. (B5) produces six terms, the second and the third give two and one terms respectively, which overall results in nine terms represented by the diagrams shown in Fig. 3. This nine term expression connects the polarization $\alpha^{(3)}(\tau)$ to the driving field $F(\tau)$.

APPENDIX C: TIME-ORDERED EXPRESSION FOR $R^{(7)}$

To recast the response function $R^{(7)}(t;\tau_3,\tau_2,\tau_1)$ derived in Appendix B for time-ordered variables $\tau_3>\tau_2>\tau_1$ we represent the driving field in a form

$$F(\tau)=\bar{F}_1\delta(\tau-\tau_1)+\bar{F}_2\delta(\tau-\tau_2)+\bar{F}_3\delta(\tau-\tau_3), \tag{C1}$$

and denote the contribution to $\alpha^{(3)}(t)$ proportional to $\bar{F}_1\bar{F}_2\bar{F}_3$ by $\bar{\alpha}^{(3)}(t)$. Making use of Eq. (2.12) we obtain

$$\bar{\alpha}^{(3)}(t)=R^{(7)}(t;\tau_3,\tau_2,\tau_1)\bar{F}_1\bar{F}_2\bar{F}_3, \tag{C2}$$

which yields the response function $R^{(7)}$ in a form

$$R^{(7)}(t;\tau_3,\tau_2,\tau_1)=\sum_{\alpha=1}^{5}R_\alpha^{(7)}(t;\tau_3,\tau_2,\tau_1)+\sum_{\alpha=6}^{9}\sum_{\beta=1}^{3}R_{\alpha\beta}^{(7)}(t;\tau_3,\tau_2,\tau_1). \tag{C3}$$

The contributions to the first sum are:

$$R_1^{(7)}(t;\tau_3,\tau_2,\tau_1)=\sum\alpha_{i_1i_2i_3}^{(3)}\alpha_{j_1}^{(1)}\alpha_{j_2}^{(1)}\alpha_{j_3}^{(1)}C_{i_1j_1}(t-\tau_1)\times C_{i_2j_2}(t-\tau_2)C_{i_3j_3}(t-\tau_3), \tag{C4}$$

$$R_2^{(7)}(t;\tau_3,\tau_2,\tau_1) = -\sum \int_{\tau_1}^{t} d\tau' V^{(4)}_{i_1 i_2 i_3 k'} \times \alpha_k^{(1)} \alpha_{j_1}^{(1)} \alpha_{j_2}^{(1)} \alpha_{j_3}^{(1)} C_{kk'}(t-\tau') \times C_{i_1 j_1}(\tau'-\tau_1) C_{i_2 j_2}(\tau'-\tau_2) \times C_{i_3 j_3}(\tau'-\tau_3), \quad \text{(C5)}$$

$$R_3^{(7)}(t;\tau_3,\tau_2,\tau_1) = -\sum \int_{\tau_1}^{\tau_3} d\tau' V_{i_1 i_2 m'} \alpha^{(2)}_{k' m} \alpha_k^{(1)} \alpha_{j_1}^{(1)} \times \alpha_{j_2}^{(1)} C_{kk'}(t-\tau_3) C_{mm'}(\tau_3-\tau') \times C_{i_1 j_1}(\tau'-\tau_1) C_{i_2 j_2}(\tau'-\tau_2), \quad \text{(C6)}$$

$$R_4^{(7)}(t;\tau_3,\tau_2,\tau_1) = \sum \alpha^{(2)}_{mk'} \alpha^{(2)}_{im'} \alpha_k^{(1)} \alpha_{i'}^{(1)} C_{kk'}(t-\tau_3) \times C_{mm'}(\tau_3-\tau_2) C_{ii'}(\tau_2-\tau_1), \quad \text{(C7)}$$

$$R_5^{(7)}(t;\tau_3,\tau_2,\tau_1) = \sum \alpha^{(3)}_{i_1 i_2 k'} \alpha_k^{(1)} \alpha_{j_1}^{(1)} \alpha_{j_2}^{(1)} \times C_{kk'}(t-\tau_3) C_{i_1 j_1}(\tau_3-\tau_1) \times C_{i_2 j_2}(\tau_3-\tau_2). \quad \text{(C8)}$$

For the second sum we need only four basic terms (with $\beta=1$),

$$R_{6,1}^{(7)}(t;\tau_3,\tau_2,\tau_1) = -\sum \int_{\tau_2}^{t} d\tau' V^{(3)}_{i_1 i_2 k'} \times \alpha^{(2)}_{i_3 k} \alpha_{j_1}^{(1)} \alpha_{j_2}^{(1)} \alpha_{j_3}^{(1)} C_{kk'}(t-\tau') \times C_{i_2 j_3}(t-\tau_3) C_{i_2 j_2}(\tau'-\tau_2) \times C_{i_1 j_1}(\tau'-\tau_1), \quad \text{(C9)}$$

$$R_{7,1}^{(7)}(t,\tau_3,\tau_2,\tau_1) = \sum \alpha^{(2)}_{i_3 k} \alpha^{(2)}_{i_1 k'} \alpha_{j_1}^{(1)} \alpha_{j_3}^{(1)} C_{i_3 j_3}(t-\tau_3) \times C_{kk'}(t-\tau_2) C_{i_1 j_1}(\tau_2-\tau_1), \quad \text{(C10)}$$

$$R_{8,1}^{(7)}(t;\tau_3,\tau_2,\tau_1) = \sum \int_{\tau_2}^{t} d\tau' \int_{\tau'}^{t} d\tau'' V^{(3)}_{m i_3 k'} V^{(3)}_{i_1 i_2 m'} \times \alpha_k^{(1)} \alpha_{j_1}^{(1)} \alpha_{j_2}^{(1)} \alpha_{j_3}^{(1)} C_{kk'}(t-\tau'') \times C_{mm'}(\tau''-\tau') C_{i_3 j_3}(\tau''-\tau_1) \times C_{i_1 j_1}(\tau'-\tau_1) C_{i_2 j_2}(\tau'-\tau_2), \quad \text{(C11)}$$

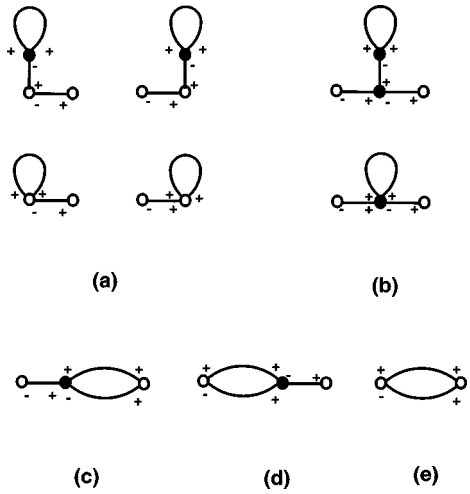

FIG. 4. Diagrammatic representation of the quantum corrections to $R^{(3)}$ to first order in $\hbar$. Line with minus and plus at the ends denote $G^{(-)}$; lines with pluses at both ends stands for $G^{(+)}$.

$$R_{9,1}^{(7)}(t;\tau_3,\tau_2,\tau_1) = -\sum \int_{\tau_2}^{t} d\tau' V^{(3)}_{i_3 m k'} \times \alpha^{(2)}_{i_1 m'} \alpha_k^{(1)} \alpha_{j_1}^{(1)} \alpha_{j_3}^{(1)} C_{kk'}(t-\tau') \times C_{i_3 j_3}(\tau'-\tau_3) C_{mm'}(\tau'-\tau_2) \times C_{i_1 j_1}(\tau_2-\tau_1). \quad \text{(C12)}$$

The remaining ($\beta=2,3$) terms in the second sum can be obtained by a simple permutation of the time arguments

$$R_{\alpha,2}^{(7)}(t;\tau_3,\tau_2,\tau_1) \equiv R_{\alpha,1}^{(7)}(t;\tau_1,\tau_3,\tau_2), \quad \text{(C13)}$$

$$R_{\alpha,3}^{(7)}(t;\tau_3,\tau_2,\tau_1) \equiv R_{\alpha,1}^{(7)}(t;\tau_2,\tau_3,\tau_1), \quad \alpha=6,7,8,9. \quad \text{(C14)}$$

APPENDIX D: QUANTUM CORRECTIONS TO $R^{(3)}$

In this Appendix we calculate the correction $\Delta R^{(3)}$ to the third-order response function to first order in $\hbar$. Corrections to higher-order response functions $R^{(2n+1)}$ as well as higher-order terms in $\hbar$ can be obtained in a similar way.

$\Delta R^{(3)}$ contains nine terms represented by the single loop diagrams shown in Fig. 4. These contributions can be naturally combined into five groups shown in Figs. 4(a)–4(e) and denoted by $\Delta R_\alpha,^{(3)}$ $\alpha=1,\ldots,5$:

$$\Delta R^{(3)}(t;\tau) = \sum_{\alpha=1}^{5} \Delta R_\alpha^{(3)}(t,\tau). \quad \text{(D1)}$$

The first term $\Delta R_1^{(3)}$ represented by diagrams given in Fig. 4(a) has the same dependence on $(t-\tau)$ as its classical counterpart given by Eq. (4.1). A straightforward calculation gives

$$\Delta R_1^{(3)}(t;\tau) = \hbar \sum_{mn} Z_{mn}^{(1)} C_{mn}(t-\tau), \quad \text{(D2)}$$

with

$$Z^{(1)}_{mn} \equiv -\frac{1}{2}\sum_{pqrj}(\alpha^{(2)}_{jn}\alpha^{(1)}_{m}+\alpha^{(2)}_{jm}\alpha^{(1)}_{n})V^{(3)}_{pqr}C^{(+)}_{pq}(0) \times \int_0^\infty d\tau' C_{jr}(\tau')+\frac{1}{2}\sum_{pq}(\alpha^{(3)}_{pqn}\alpha^{(1)}_{m} + \alpha^{(3)}_{pqm}\alpha^{(1)}_{n})C^{(+)}_{pq}(0). \quad \text{(D3)}$$

Here we have introduced the notation

$$C^{(+)}_{ij}(\tau) \equiv \int_{-\infty}^{\infty}\frac{d\omega}{2\pi}C_{ij}(\omega)\coth\left(\frac{\omega}{2\omega_T}\right)cos(\omega\tau), \quad \text{(D4)}$$

and in particular

$$C^{(+)}_{ij}(0) = \int_{-\infty}^{\infty}\frac{d\omega}{2\pi}C_{ij}(\omega)\coth\left(\frac{\omega}{2\omega_T}\right). \quad \text{(D5)}$$

Equations (D1)–(D4) show that $\Delta R^{(3)}_1$ does depend on temperature. It is clearly seen from Fig. 4(a) that $\Delta R^{(3)}_1$ reflects quantum corrections to the polarization operator originating from anharmonicities in the Hamiltonian and nonlinearities in the expansion of the polarization in nuclear coordinates. $\Delta R^{(3)}_1$ also accounts for deviations of the initial equilibrium state from the harmonic approximation due to the anharmonicities.

$\Delta R^{(3)}_2$ represented diagrammatically in Fig. 4(b) constitutes a correction to the response function due to self-energies of nuclear motions induced by anharmonicities. A straightforward calculation yields

$$\Delta R^{(3)}_2(t;\tau) = \hbar\sum_{ijmn}\alpha^{(1)}_i\alpha^{(1)}_j\Sigma^{(1)}_{nm}\int_\tau^t d\tau' \times C_{in}(t-\tau')C_{mj}(\tau'-\tau), \quad \text{(D6)}$$

with the self-energy

$$\Sigma^{(1)}_{nm} \equiv \frac{1}{2}\sum_{pqrs}V^{(3)}_{mnq}V^{(3)}_{prs}C^{(+)}_{pr}(0)\int_0^\infty d\tau' C_{qs}(\tau') - \frac{1}{2}\sum_{pq}V^{(4)}_{mnpq}C^{(+)}_{pq}(0). \quad \text{(D7)}$$

The contributions $R^{(3)}_\alpha(t;\tau)$ for $\alpha = 3,4,5$ represented in Figs. 4(c), 4(e), and 4(e) respectively constitute new types of quantum corrections which may not be introduced through self-energies or renormalization of overall factors. They are given by:

$$\Delta R^{(3)}_3(t;\tau) = -\hbar\sum\alpha^{(1)}_i\alpha^{(2)}_{js}V^{(3)}_{mnq}\int_\tau^t d\tau' C_{jn}(t-\tau') \times C^{(+)}_{sm}(t-\tau')C_{qi}(\tau'-\tau), \quad \text{(D8)}$$

and

$$\Delta R^{(3)}_4(t;\tau) = -\hbar\sum\alpha^{(1)}_i\alpha^{(2)}_{js}V^{(3)}_{mnq}\int_\tau^t d\tau' C_{iq}(t-\tau') \times C_{ns}(\tau'-\tau)C^{(+)}_{mj}(\tau'-\tau), \quad \text{(D9)}$$

$$\Delta R^{(3)}_5(t;\tau) = \hbar\sum\alpha^{(2)}_{ij}\alpha^{(2)}_{mn}C^{(+)}_{mi}(t-\tau)C_{nj}(t-\tau). \quad \text{(D10)}$$

Here Σ stands for a summation over all repeating indices.

[1] *Proceedings of Time Resolved Vibrational Spectroscopy VIII*, edited by T. Parker, Laser Chemistry (1998).
[2] A. Laubereau and W. Kaiser, Rev. Mod. Phys. **50**, 607 (1978); W. Zinth, M. C. , and W. Kaiser, Phys. Rev. A **30**, 1139 (1984); W. Zinth, H.-J. Polland, A. Laubereau, and W. Kaiser, Appl. Phys. B: Photophys. Laser Chem. **26**, 77 (1982); W. Zinth, R. Leonhardt, H. Holzapfel, and W. Kaiser, IEEE J. Quantum Electron. **24**, 455 (1988).
[3] R. F. Loring and S. Mukamel, J. Chem. Phys. **83**, 2119 (1985); S. Mukamel and R. F. Loring, J. Opt. Soc. Am. B **3**, 595 (1986).
[4] R. R. Ernst, G. Bodenhausen, and A. Wokaun, *Principles of Nuclear Magnetic Resonance in One and Two Dimensions* (Clarendon, Oxford, 1987); J. K. Sanders and B. K. Hunter, *Modern NMR Spectroscopy* (Oxford, NY, 1993).
[5] B. Bechinger, M. Zasloff, and S. J. Opella, Protein Sci. **2**, 2077 (1993); A. Ramamoorthy, F. M. Marassi, and S. J. Opella, in *Dynamics and the Problem of Recognition in Biological Macromolecules*, edited by O. Jardetzky and J. Lefevre (Plenum, New York, 1996), p. 237.
[6] D. V. Bout, L. J. Muller, and M. Berg, Phys. Rev. Lett. **67**, 3700 (1991); M. Berg and D. A. V. Bout, Acc. Chem. Res. **30**, 65 (1997).
[7] K. Tominaga and K. Yoshihara, Phys. Rev. Lett. **74**, 3061 (1995); K. Tominaga, G. P. Keogh, Y. Naitoh, and K. Yoshihara, J. Raman Spectrosc. **26**, 495 (1995); K. Tominaga and K. Yoshihara, J. Chem. Phys. **104**, 1159 (1996); **104**, 4419 (1996); K. Tominaga, *Advances in Multi-Photon Processes and Spectroscopy*, *Vol. 11* (World Scientific, Singapore, 1997, in press).
[8] Y. Tanimura and S. Mukamel, J. Chem. Phys. **99**, 9496 (1993); V. Khidekel and S. Mukamel, Chem. Phys. Lett. **240**, 304 (1995); **263**, 350 (1996) (E).
[9] T. Steffen and K. Duppen, Phys. Rev. Lett. **76**, 1224 (1996); J. Chem. Phys. **106**, 3854 (1997).
[10] A. Tokmakoff and G. R. Fleming, J. Chem. Phys. **106**, 2569 (1997); A. Tokmakoff, M. J. Lang, D. S. Larsen, G. R. Fleming, Chem. Phys. Lett. (in press).
[11] A. Tokmakoff, M. J. Lang, D. S. Larsen, G. R. Fleming, V. Chernyak, and S. Mukamel, Phys. Rev. Lett. **79**, 2702 (1997).
[12] S. P. Palese, J. T. Buontempo, L. Schilling, W. T. Lotshaw, Y. Tanimura, S. Mukamel, and R. J. D. Miller, J. Phys. Chem. **98**, 12466 (1994); J. A. Leegwater and S. Mukamel, J. Chem. Phys. **102**, 2365 (1995).
[13] S. Saito and I. Ohmine, J. Chem. Phys. **108**, 240 (1998).
[14] V. Khidekel, V. Chernyak, and S. Mukamel, J. Chem. Phys. **105**, 8543 (1996).
[15] A. Tokmakoff, J. Chem. Phys. **105**, 13 (1996).
[16] T. Steffen, J. T. Fourkas, and K. Duppen, J. Chem. Phys. **105**, 7364 (1996).
[17] K. Okumura and Y. Tanimura, J. Chem. Phys. **105**, 7294 (1996); **106**, 1687 (1997).
[18] L. D. Landau and E. M. Lifshitz, *Quantum Mechanics* (Pergamon, New York, 1977).
[19] S. Mukamel, V. Khidekel, and V. Chernyak, Phys. Rev. E **53**, 1 (1996).
[20] F. Barocchi, M. Neumann, and M. Zoppi, Phys. Rev. A **36**, 2440 (1987); F. Barocchi, M. Zoppi, and M. Neumann, *ibid.* **27**, 1587 (1983).
[21] V. Khidekel, V. Chernyak, and S. Mukamel, *Femtochemistry*, edited by M. Chergui (World Scientific, Singapore, 1996), p. 507.
[22] S. Mukamel, *Principles of Nonlinear Optical Spectroscopy* (Oxford University Press, New York, 1995).
[23] R. W. Hellwarth, Prog. Quantum Electron. **5**, 2 (1977).
[24] V. Chernyak, N. Wang, and S. Mukamel, Phys. Rep. **263**, 213 (1995).
[25] V. Chernyak and S. Mukamel, J. Chem. Phys. **105**, 4565 (1996).
[26] A. A. Abrikosov, L. P. Gorkov, and I. Ye, *Dzyaloshinsky*, *Quantum Field Theoretical Methods in Statistical Physics* (Oxford University Press, New York 1965); L. P. Kadanoff and G. Baym, *Quantum Statistical Mechanics* (Benjamin, New York, 1962); G. D. Mahan, *Many-Particle Physics* (Plenum, New York 1990).
[27] L. V. Keldysh, Zh. Éksp Teor. Fiz. **47**, 1515 (1964) [Sov. Phys. JETP **20**, 1018 (1965)]; J. Schwinger, J. Math. Phys. **2**, 407 (1961); E. M. Lifshitz and L. P. Pitaevsky, *Physical Kinetics* (Pergamon, Oxford, 1981).
[28] B. S. DeWitt, *Dynamical Theory of Groups and Fields* (Gordon and Breach, New York, 1965).
[29] H. Haug and S. W. Koch, *Quantum Theory of the Optical and Electronic Properties of Semiconductors* (World Scientific, Singapore, 1990).
[30] S. Mukamel, S. Tretiak, T. Wagersreiter, and V. Chernyak, Science **277**, 781 (1997).
[31] L. R. Narasimhan, K. A. Littau, D. W. Pack, Y. S. Bai, A. Elschner, and M. D. Fayer, Chem. Rev. **90**, 439 (1990); C. W. Rella, A. Kwok, K.

Rector, J. R. Hill, H. A. Schwettman, D. D. Dlott, and M. D. Fayer, Phys. Rev. Lett. **77**, 1648 (1996).
[32] T. E. Creighton, *Proteins: Structures and Molecular Properties*, 2nd ed. (Freeman, New York, 1993).
[33] B. Locke, R. Diller, and R. M. Hochstrasser, in *Biomolecular Spectroscopy*, edited by R. J. H. Clark and R. E. Hester (Wiley, New York, 1993); R. M. Hochstrasser, private communication.
[34] D. T. Lesson and D. A. Wiersma, Phys. Rev. Lett. **74**, 2138 (1995); D. T. Lesson, D. A. Wiersma, K. Fritsch, and J. Friedrich, J. Phys. Chem. **101**, 6331 (1997).
[35] Y. J. Yan and S. Mukamel, J. Chem. Phys. **88**, 5735 (1988).
[36] V. Chernyak and S. Mukamel, J. Chem. Phys. **104**, 444 (1996).
[37] T. Meier and S. Mukamel, Phys. Rev. Lett. **77**, 3471 (1996); T. Meier, S. Tretiak, V. Chernyak, and S. Mukamel, Phys. Rev. B **55**, 4960 (1997).